Development 134, 2673-2684 (2007) doi:10.1242/dev.02865

Retinoic acid counteracts developmental defects in the substantia nigra caused by Pitx3 deficiency

Frank M. J. Jacobs*, Simone M. Smits*, Cornelle W. Noorlander, Lars von Oerthel, Annemarie J. A. van der Linden, J. Peter H. Burbach and Marten P. Smidt†

Selective neuronal loss in the substantia nigra (SNc), as described for Parkinson's disease (PD) in humans and for *Pitx3* deficiency in mice, highlights the existence of neuronal subpopulations. As yet unknown subset-specific gene cascades might underlie the observed differences in neuronal vulnerability. We identified a developmental cascade in mice in which *Ahd2* (*Aldh1a1*) is under the transcriptional control of Pitx3. Interestingly, Ahd2 distribution is restricted to a subpopulation of the meso-diencephalic dopaminergic (mdDA) neurons that is affected by *Pitx3* deficiency. Ahd2 is involved in the synthesis of retinoic acid (RA), which has a crucial role in neuronal patterning, differentiation and survival in the brain. Most intriguingly, restoring RA signaling in the embryonic mdDA area counteracts the developmental defects caused by *Pitx3* deficiency. The number of tyrosine hydroxylase-positive (TH+) neurons was significantly increased after RA treatment in the rostral mdDA region of *Pitx3*$^{-/-}$ embryos. This effect was specific for the rostral part of the developing mdDA area, and was observed exclusively in *Pitx3*$^{-/-}$ embryos. The effect of RA treatment during the critical phase was preserved until later in development, and our data suggest that RA is required for the establishment of proper mdDA neuronal identity. This positions Pitx3 centrally in a mdDA developmental cascade linked to RA signaling. Here, we propose a novel mechanism in which RA is involved in mdDA neuronal development and maintenance, providing new insights into subset-specific vulnerability in PD.

KEY WORDS: Pitx3, Retinoic acid, Aldehyde dehydrogenase, Development, Midbrain, Dopamine, Parkinson's disease, Ahd2, aldh1a1, Mouse

INTRODUCTION

Parkinson's disease (PD) is a common progressive neurodegenerative movement disorder attributed to selective loss of pigmented dopaminergic (DA) neurons in the substantia nigra pars compacta (SNc). Interestingly, adjacent DA neurons located in the ventral tegmental area (VTA) are largely spared (Hirsch et al., 1988). Analysis of animal models for PD demonstrates a similar susceptibility to degeneration of SNc DA neurons, indicating a conserved phenomenon among species (Blum et al., 2001). Although several genes have now been associated with PD (Moore et al., 2005; Abou-Sleiman, 2006), the exact mechanism underlying the specific degeneration of DA neurons located in the SNc is not fully understood.

The homeodomain transcription factor Pitx3, exclusively expressed in meso-diencephalic DA (mdDA) neurons in the brain (Smidt et al., 1997), is essential for the proper development of the mdDA system. Analysis of *Pitx3*-deficient mice has revealed that the loss of Pitx3 expression leads to the selective loss of a neuronal subset located primarily in the SNc (Hwang et al., 2003; Nunes et al., 2003; van den Munckhof et al., 2003; Smidt et al., 2004a; Smidt et al., 2004b). The mechanism by which Pitx3 influences the development of this specific mdDA subpopulation is still unknown. Although *Pitx3* deficiency results in early developmental defects of mdDA neurons, whereas PD is a progressive neurodegenerative disease with late onset, both affect the same mdDA neuronal population. Therefore, knowledge of molecular pathways controlled by Pitx3 might provide new insights into mdDA pathology, as in PD. However, until now, no target genes of Pitx3 have been identified, although some genes are associated with Pitx3 function (Smits et al., 2006). One of these genes encodes the enzyme aldehyde dehydrogenase family 1, subfamily A1 (Aldh1a1; also known as Raldh1 or Ahd2). In embryonic stem (ES) cells, transgenic expression of Pitx3 leads to an increased ratio of ES cells that are positive for both Ahd2 and tyrosine hydroxylase (Ahd2+/TH+) (Chung et al., 2005). Although this suggests a relationship between Pitx3 and Ahd2 expression, a relatively large portion of cells (approximately 70%) that were positive for both Pitx3 and TH still showed no induction of Ahd2.

In mice, Ahd2 is first detected in the mesencephalic flexure as early as embryonic day (E)9 (Haselbeck et al., 1999; Westerlund et al., 2005). There is, however, a marked change in Ahd2 distribution during different stages of development within this area. From E9 until E11.5, Ahd2 is found in a broad area ranging from the ventricular zone to the most ventral neuronal population within the mantle layer (Wallen et al., 1999). By contrast, from E12.5 onwards, Ahd2 distribution is largely confined to a selective subpopulation of mdDA neurons in a rostro-ventral portion of the mdDA area (McCaffery and Drager, 1994; Wallen et al., 1999; Chung et al., 2005). These data suggest that Ahd2 has a dual role in the presumptive mdDA area throughout development, functioning both in the proliferative and migratory stages, and during the final differentiation and maintenance of a selective mdDA neuronal subpopulation. Ahd2 is involved in the production of retinoic acid (RA) from retinol, which is crucial for neuronal patterning and differentiation (Duester, 2000; McCaffery et al., 2003). Via binding to the RA receptor (RAR) and retinoid X receptor (RXR), RA has been shown to induce tissue-specific gene transcription leading to cellular differentiation (Chambon, 1996). RA is detected in the midbrain area during early embryonic stages (Niederreither et al.,

Rudolf Magnus Institute of Neuroscience, Department of Pharmacology and Anatomy, University Medical Center Utrecht, Universiteitsweg 100, 3584 CG Utrecht, The Netherlands.

*These authors contributed equally to this work and should be considered shared first author
†Author for correspondence (e-mail: m.p.smidt-2@umcutrecht.nl)

Accepted 3 May 2007

2002a), and in the postnatal and adult brain (McGaffery and Drager, 1994). Interestingly, Ahd2 is the only aldehyde dehydrogenase present in the mdDA area during the developmental and adult stage (Niederreither et al., 2002b), suggesting an important role for Ahd2-mediated RA production in the mdDA system.

Based on the restricted expression pattern of Ahd2 within the mdDA neuronal population, together with the implicated relationship between Pitx3 and Ahd2 in ES cells, we studied the relationship between Pitx3 and Ahd2 in more detail in mdDA neurons. Our results show that Pitx3 regulates *Ahd2* expression both in vivo and in vitro. Furthermore, Pitx3 interacts with a highly conserved region in the proximity of the transcriptional start site of the *Ahd2* gene, suggesting that Pitx3 activates *Ahd2* directly at the transcriptional level. Most intriguingly, we show that maternal supplementation of RA counteracts the developmental defects caused by *Pitx3* deficiency in a specific mdDA neuronal subpopulation. In this study, we provide evidence for the existence of a developmental cascade in which Pitx3 is positioned centrally in RA-dependent final differentiation of mdDA neurons.

MATERIALS AND METHODS

Animals

Experiments were carried out in *Pitx3*-deficient mice from two different breeding strategies. Adult C57Bl/6-Jico wild-type mice (Charles River Laboratories, France) and Aphakia (ak) mice, which have been described previously (Semina et al., 2000; Rieger et al., 2001; Smidt et al., 2004a) were used in homozygous breeding. In heterozygous breeding, male ak mice were crossed to female C57BL/6-Jola mice to generate heterozygous F1 hybrids. F1 hybrids were intercrossed to generate $Pitx3^{+/+}$, $Pitx3^{+/-}$ and $Pitx3^{-/-}$ progeny. Genotypes were determined by PCR analysis of tail DNA. Pregnant mice were decapitated or euthanized by CO_2 asphyxiation and embryos were collected at E13.5, E14.5 or E18.5 (the day on which the copulatory plug was detected was considered E0). Adult mice were euthanized by CO_2 asphyxiation and brains were collected. Mice were bred in our laboratory under standard conditions (21.0±1.0°C and 50% humidity) with ad libitum access to standard food (Hope Farms) and tap water, on a 12:12 hour light:dark cycle. All experimental procedures were approved by the ethical committee for animal experimentation of the Utrecht University, the Netherlands.

In situ hybridization

Embryos and adult brains were collected and immediately frozen on dry ice. Sections (16 μm) were cut and collected on SuperFrost Plus slides (Menzel Gläser). In situ hybridization (ISH) with digoxigenin (DIG)-labeled and [^{33}P]-labeled cRNA probes was performed as described previously (Smidt et al., 2004a; Smits et al., 2005). [^{33}P]-labeled sections were dehydrated, air-dried and exposed to BAS-MS 2340 imaging plates (Fuji) for 3-5 days or to Kodak Biomax MR films (Kodak) for 3 weeks. Autoradiographic BAS-MS 2340 imaging plates containing the hybridization signals were scanned using the FLA-5000 imaging system (Fuji), and quantitative analysis was performed using the AIDA Image Analyzer Software (Raytest). Gene expression was analyzed in both the left and right SNc ($Pitx3^{+/+}$: n=8; $Pitx3^{+/-}$: n=5). Per animal, two adjacent sections in the SNc were analyzed. To evaluate statistical significance, data were subjected to the Student's t-test (two tailed). The following probes were used: a 1142 bp fragment of the rat *Th* cDNA (Grima et al., 1985), an *Aadc* (also known as *Ddc* – Mouse Genome Informatics) fragment containing bp 22-488 of the mouse coding sequence (Smits et al., 2003), a fragment containing bp 290-799 of the coding region from the mouse *Vmat2* (also known as *Slc18a2* – Mouse Genome Informatics) gene (Smits et al., 2003), an alpha-synuclein (a-synuclein; *Snca*) fragment containing bp 20-420 of the coding region from the mouse cDNA (Smidt et al., 2004a), and an *Ahd2* fragment containing bp 568-1392 of the mouse coding sequence.

Immunohistochemistry

Embryos and adult brains were collected, incubated overnight in 4% paraformaldehyde (PFA) at 4°C, and embedded in paraffin. Sections (7 μm) were cut on a microtome, collected on SuperFrost Plus slides (Menzel Gläser), de-paraffinated through xylene, rehydrated through an ethanol series and incubated in 0.3% H_2O_2 in Tris-buffered saline (TBS) for 30 minutes. Next, sections were boiled in citrate buffer (pH 6) for antigen retrieval, blocked with 4% fetal calf serum in TBS for 30 minutes and incubated overnight with rabbit anti-TH antibody (Pel-Freez, Arkansas, USA; 1:1000) in TBS/0.5% Triton at 4°C. The next day, sections were incubated for 1 hour with biotinylated goat anti-rabbit immunoglobulin in TBS (1:1000), followed by incubation with avidin-biotin-peroxidase reagents (ABC elite kit, Vector Laboratories, 1:1000) for 1 hour in TBS. The slides were stained with DAB (3,3′-diamino-benzidine) for a maximum of 10 minutes, until the background was lightly stained. Slides were dehydrated with ethanol and mounted using Entellan. Quantification of neurons was performed using a microscope (Zeiss Axiovert 405M) attached to a camera system (MicroPublisher 5.0 RTV) and imaging software (Openlab 5.0.1, Improvision). The number of TH-immunoreactive (TH-IR) neurons was counted unilaterally in anatomically matched adjacent coronal sections. For each E14.5 embryo, four sections were counted in the caudal and rostral domain of the mdDA system. For each E18.5 embryo, sections containing the SNc were analyzed (27-40 sections) and the average number of TH-IR neurons per section was calculated. Only neurons in which cell nuclei could be recognized were counted. Quantification was performed by an independent observer in a blind design. To evaluate statistical significance, data were subjected to the Student's t-test (two tailed).

For double-immunofluorescence staining, sections were incubated overnight with rabbit anti-Ahd2 (Abcam, diluted 1:100) in combination with sheep anti-TH (Chemicon, diluted 1:500) in PBS/0.5% Triton at 4°C. The next day, sections were incubated with fluorophore-conjugated secondary antibodies in PBS (Alexa-Fluor-488-conjugated goat anti-rabbit and Alexa-Fluor-555-conjugated donkey anti-sheep, diluted 1:400; Molecular Probes) for 1 hour at room temperature and embedded with 90% glycerol.

Nissl staining

TH-IR sections were counterstained for 5 minutes in 0.5% cresyl violet and briefly rinsed in an acetate buffer (pH 4). The sections were then differentiated in 96% ethanol for 60 seconds, dehydrated in 100% ethanol, cleared in xylene and mounted with Entellan. Neuronal number per section in the rostral mdDA area was determined in cresyl violet-stained sections, delineated according to TH-IR area. Quantification (n=3) was performed by an independent observer in a blind design. To evaluate statistical significance, data were subjected to the Student's t-test (two tailed).

Combined ISH-immunohistochemistry

Adult brains were collected, incubated overnight in 4% PFA at 4°C, and embedded in paraffin. Sections (7 μm) were cut and collected on SuperFrost Plus slides (Menzel Gläser). ISH on paraffin wax sections was performed as described for frozen sections with the following modifications: sections were first deparaffinated through xylene, rehydrated through an ethanol series, boiled in citrate buffer (pH 6), and incubated in 0.2 M HCl for 15 minutes. Sections were further treated as described above for DIG-ISH on frozen sections, except that, after termination of the alkaline phosphatase reaction, sections were immunostained for TH with the avidin-biotin-peroxidase complex (ABC) method, as described above.

RNA isolation, PCR and cloning

RNA from E18 mouse whole brain or MN9D cells was isolated using Trizol (Invitrogen) according the manufacturer's guidelines. A sample of $Pitx3^{+/GFP}$ FACS-sorted mdDA cells from E16 embryos was isolated via the guanidine thiocyanate method.

Full-length *Pitx3* cDNA was amplified from cDNA originating from E18 whole-brain RNA, with the following primers: forward, 5′-CCCTG-CCTGCGCTCCAGAAC-3′; reversed: 5′-CCCTGTTCCTGGCCTTA-GTC-3′. *Pitx3* was ligated in pGEM-T easy vector (Promega) for sequence analysis, and subsequently cloned into pcDNA3.1(–) vector (Invitrogen) using the *Apa*I and *Bstx*I restriction sites.

To distinguish between the *Ahd2* and *Aldh1a7* genes, primers with 100% homology to both genes were designed: forward, 5′-GACTGATGAG-ATGCGCATTG-3′; reversed 5′-GTCTTGAGCTCAGTGTATTC-3′. For in vivo determination, RNA originating from E16 ventral midbrain $Pitx3^{+/GFP}$ cells was subjected to OneStep reverse transcriptase (RT)-PCR (Qiagen). For

in vitro determination, RNA from MN9D cells transfected with *Pitx3*-pcDNA3.1 was used. The obtained PCR fragments were cloned into pGEM-T easy vectors and eight different clones of each cloning were sequence-analyzed (Baseclear, The Netherlands).

MN9D cell culture and cell transfections

MN9D (MN9D-13N) cells were cultured in Dulbecco's Modified Eagle Medium (DMEM) supplemented with 10% (v/v) hiFCS, 100 units/ml penicillin, 100 units/ml streptomycin and 2 mM L-glutamine in a humidified atmosphere with 5% CO_2 at 37°C. Cells were grown on 10-cm-diameter dishes coated with poly L-lysine. At 2 hours prior to transfection, culture medium was replaced with medium without antibiotics, and transfection was performed using Lipofectamine 2000 (Invitrogen), according to the manufacturer's guidelines. Cells were transfected with 5 μg of *Pitx3*-pcDNA3.1 or an equal molar amount of empty pcDNA3.1 vector together with carrier DNA and 1 μg of EGFP-N1 vector (Clontech). At 6 hours after transfection, cells were divided and allowed to grow for an additional 30 hours. Transfection efficiency was determined based on GFP fluorescence using a fluorescent microscope, and plates were matched based on their relative transfection efficiency. For MN9D cells, a typical transfection efficiency with Lipofectamine is approximately 80-90%. Finally, cells were harvested for RNA isolation or used for a chromatin immunoprecipitation assay.

Semi-quantitative RT-PCR

Relative gene expression levels were determined using a OneStep RT-PCR kit (Qiagen). We used 50 ng total RNA per reaction, and for each transcript the linear phase was determined and reactions were stopped during that phase for analysis (for primer sequences, see Table 1). Samples were loaded on 2% agarose gels and, after gel electroforesis, gels were scanned using a FLA-5000 imaging system (Fuji) and relative amounts of DNA were measured with a densitometer. Each analysis was replicated at least three times with independent RNA samples to confirm the obtained results. To determine whether RA regulates the expression of TH, we cultured MN9D cells in the presence of 1 μM all-trans RA for 36 hours as described previously (Castro et al., 2001).

Chromatin immunoprecipitation (ChIP) assay

MN9D cells were transfected with *Pitx3*-pcDNA3.1 or empty pcDNA3.1 expression vector at 90% confluence. At 6 hours after transfection, cells were divided and allowed to grow for an additional 30 hours. Formaldehyde was added directly to the medium to a final concentration of 1%, and cells were incubated at room temperature for 10 minutes. Glycine was added to a final concentration of 0.125 M, and cells were incubated at room temperature for an additional 5 minutes. Cells were washed twice with PBS, harvested and pelleted by centrifugation. ChIP was performed as described previously (Matthews et al., 2005), with some adjustments. Cells were resuspended in lysis buffer [50 mM Tris-HCl (pH 8.0), 150 mM NaCl, 1 mM EDTA, 1% Triton X-100, 0.1% Na-deoxycholate] containing protease inhibitors (Complete Protease Inhibitor Cocktail Tablets, Roche) and were incubated on ice for 20 minutes. Subsequently, the lysate was put through a 27/3-4 G syringe three times. Chromatin was sonicated using a Soniprep 150 sonicator to obtain DNA of an average length of 400-500 bp. Chromatin was pre-cleared with 60 μl of a 50% slurry of Protein A agarose/Salmon Sperm DNA (Upstate) for 1.5 hours at 4°C. Pre-cleared chromatin was incubated overnight with approximately 1 μg of Pitx3 antibody (Smidt et al., 2000), or with 1 μg of rabbit whole serum immunoglobulins (Sigma) as a negative control. Antibody-DNA complexes were captured by adding 20 μl of a 50% slurry of Protein A agarose/Salmon Sperm DNA for 1 hour at 4°C. Immunoprecipitated complexes were washed for 10 minutes with the following wash buffers: twice with 1.5 ml of buffer 1 [20 mM Tris-HCl (pH 8.0), 150 mM NaCl, 2 mM EDTA, 1% Triton X-100, 0.1% sodium dodecyl sulfate (SDS)], once with 1.5 ml of buffer 2 [20 mM Tris-HCl (pH 8.0), 500 mM NaCl, 2 mM EDTA, 1% Triton X-100, 0.1% SDS], once with 1.5 ml of LiCl buffer [20 mM Tris-HCl (pH 8.0), 250 mM LiCl, 1 mM EDTA, 1% NP-40, 1% Na-deoxycholate], and twice with 1.5 ml of TE [10 mM Tris-HCl (pH 8.0), 1 mM EDTA]. For elution of the immunocomplexes, 150 μl of elution buffer (TE, 1% SDS) was added and beads were shaken on a vortex for 30 minutes at 4°C. This was performed twice and samples were pooled. Crosslinks were reversed overnight at 67°C and complexes were precipitated and dissolved in TE. Proteinase K was added and samples were incubated for 2 hours at 45°C. Samples were extracted once with phenol/chloroform (1:1) and twice with chloroform. DNA was precipitated and dissolved in 100 μl of PCR grade MilliQ. For each PCR reaction, 2 μl of this DNA sample was used (for primer sequences, see Table 1).

Retinoic acid treatment of pregnant *Pitx3*$^{+/-}$ mice

Following timed matings of *Pitx3*$^{+/-}$ parents, pregnant mice were supplemented with all-trans-RA (Sigma), which will be referred to as RA in this article, twice daily from E10.75 to E13.75. RA was dissolved in corn-oil and mixed with powdered food to a final concentration of 0.25 mg/g food, which was supplied ad libitum as previously described (Niederreither et al., 2002c; Mic et al., 2003). RA was dissolved freshly each time and supplemented food was supplied at 12-hour intervals. The control *Pitx3*$^{+/-}$ animals were treated according to the same protocol, but were supplemented with corn oil without RA. Embryos were isolated at E14.5 and E18.5, and weight-matched *Pitx3*$^{+/+}$ and *Pitx3*$^{-/-}$ littermates were analyzed by immunohistochemistry.

Table 1. Primer sequences for semi-quantitative RT-PCR analysis

Fragments	Forward primer (5′→3′)	Reversed primer (5′→3′)
OneStep RT-PCR (Fig. 5)		
AADC	GAAGAGGCAAGGAGATGGTG	AACTTTAGTCCGAGCAGCCA
Ahd2	AGGCTGGGCTGACAAGATTC	AAGGCCACCTTGTCGACATC
Pitx3	CCCTCCGCTTCCAGAACATG	GTCCACACCGCGATCTCTTC
Snca	ACTTTCAAAGGCCAAGGAGG	AGGCTTCACGCTCATAGTCTTG
Tbp	GAGAATAAGAGAGCCACGGAC′	TCACATCACAGCTCCCCAC
TH	CCCACGTGGAATACACAAAG′	GAGGCATGACGGATGTACTG
Vmat2	GCAGTCACACAAGGCTACCA	TGAATAGCCCCATCCAAGAG
ChIP-assay (Fig. 6)		
Region 1	ACCCTGTTGTATCACGTATG	CAGTGTGGACTAAAAGCTAG
Region 2	CAGCCAAGTTCCAGGAGATG	GTATCTGATACAACCTGGGC
Region 3	GGAGGCAATCATGTAACTATC′	GGGGACCTCAGTAAAGAATC
Region 4	AGGGAGCATGCAAATGAAAG	AGCACCAAACAGATCCATTC
Region 5	CATCTGCTCTAGTCAGTAAG	ACAGGCATAGAGAAGGCTTC
Region 6	GAGGTAGCTGCTTAACTTAC	CCCAGGTAGTATCTTTCTTAC
Region 7	CTGTCCCCTAAATTGACAA	ATAGCCACTCTTCCTATAAC
Region 8	GGAAAGGATGTCATATAGTC	GCTCCAGAGGCTACTTCAG
Region 9	CCCTTGGACACACAGTTGTC	CAATGGCTCCCTTCTCTAATC

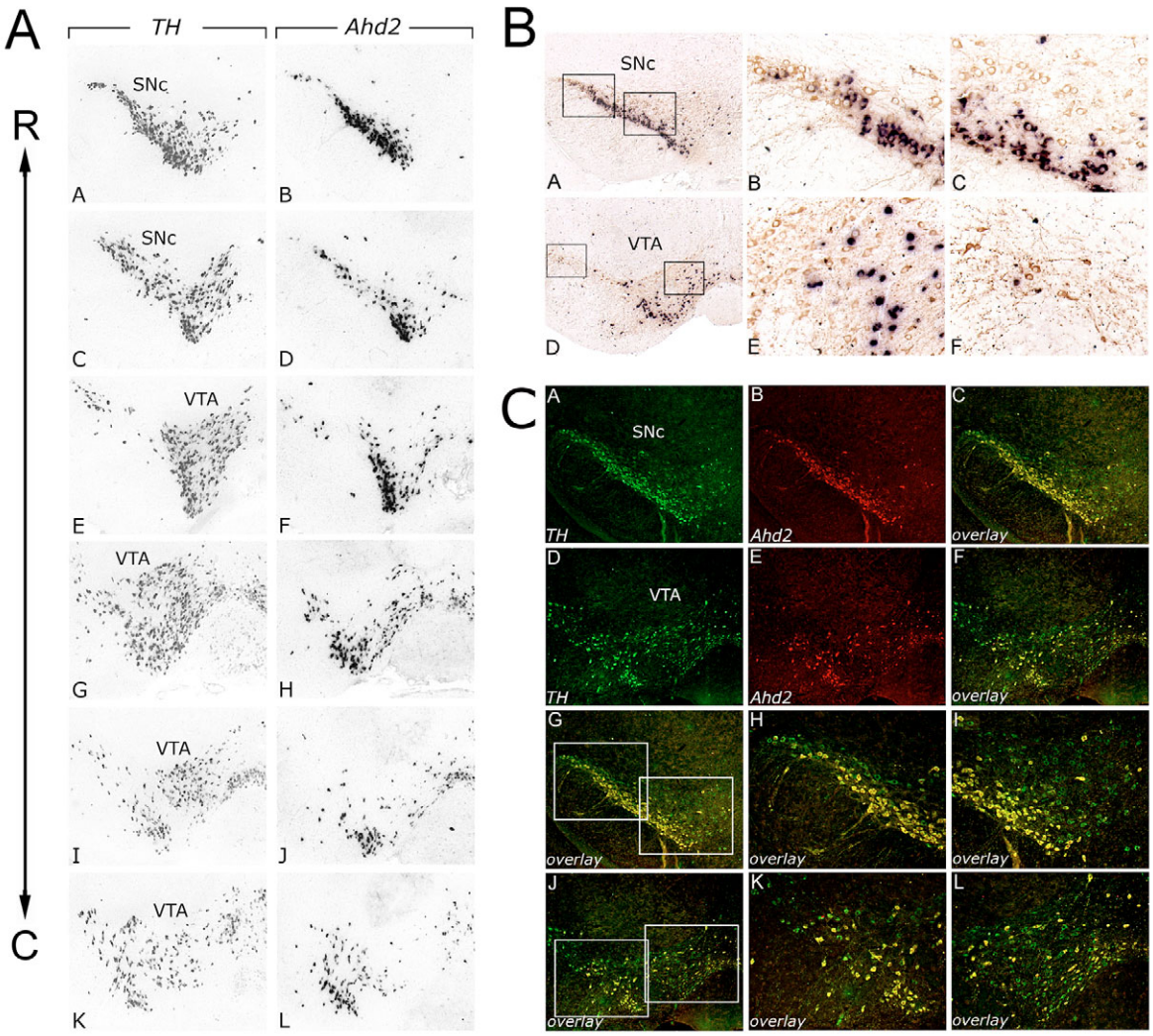

Fig. 1. Ahd2 expression marks a specific mdDA subpopulation in the adult brain. (**A**) Coronal sections from the rostral (R) to caudal (C) mdDA area containing neurons in the SNc (A-D) and VTA (E-L). (Left panels) The cell bodies of these mdDA neurons were identified by *Th* mRNA expression. (Right panels) Analysis of *Ahd2* expression on adjacent sections. (**B**) Combined in situ hybridization for *Ahd2* mRNA (purple) and an immunohistochemical staining for TH protein (brown) on adult coronal sections. The boxed areas indicated in A and D are displayed at a higher magnification in the panels B and C, and E and F, respectively. (**C**) Adult coronal sections of the SNc (A-C,G-I) and VTA (D-F,J-L). (B,E) Ahd2 protein distribution (red). MdDA neurons were identified by the expression of TH protein (green; A,D). Overlays demonstrate the co-expression of the TH and Ahd2 proteins in a subpopulation of mdDA neurons located in the SNc and VTA (C,F-L). The boxed areas indicated in G and J are displayed at a higher magnification in H and I, and K and L, respectively. mdDA, meso-diencephalic dopaminergic; SNc. substantia nigra pars compacta; VTA, ventral tegmental area.

RESULTS

Ahd2 and not *Aldh1a7* is expressed in mdDA neurons

The *Ahd2* gene displays a high degree of sequence homology to *Aldh1a7*, which is also known as *Ahd2-like* or *aldh-pb* (86% on mRNA and 96% on protein level). In contrast to Ahd2, Aldh1a7 cannot catalyze the conversion of all-trans-retinal to RA (Hsu et al., 1999; Montplaisir et al., 2002). Most previous analyses did not clearly distinguish between these two transcripts. To determine which of these genes is actually expressed in mdDA neurons, reverse transcriptase (RT)-PCR was performed on RNA of FACS-sorted Pitx3$^{+/GFP}$ mdDA neurons from E16 embryos (Zhao et al., 2004). Sequence analysis of cloned PCR products identified all clones (100%) as *Ahd2*, indicating that *Ahd2* is the predominantly expressed gene in mdDA neurons (data not shown).

Ahd2 expression marks a mdDA subpopulation in the SNc and VTA

Previous work has indicated that Ahd2 expression is relatively enriched in SNc mdDA neurons, whereas its expression in the VTA is relatively scarce (McCaffery and Drager, 1994; Chung et al., 2005). To study the expression pattern of Ahd2 in more detail, the distribution of Ahd2 was examined in adult mdDA neurons of wild-type mice (Fig. 1). High levels of *Ahd2* mRNA were observed in cells located in the SNc, as revealed by the expression pattern of *Th* on adjacent sections (Fig. 1AA-AF). In addition, a large number of *Ahd2*+ cells was observed in the VTA. These cells were predominantly located in the ventral and lateral part of the VTA, with some scattered *Ahd2*+ cells located more dorsally (Fig. 1AE-AL). Although *Ahd2* is expressed in a large number of cells in the SNc and VTA, the expression patterns of *Ahd2* and *Th* did not

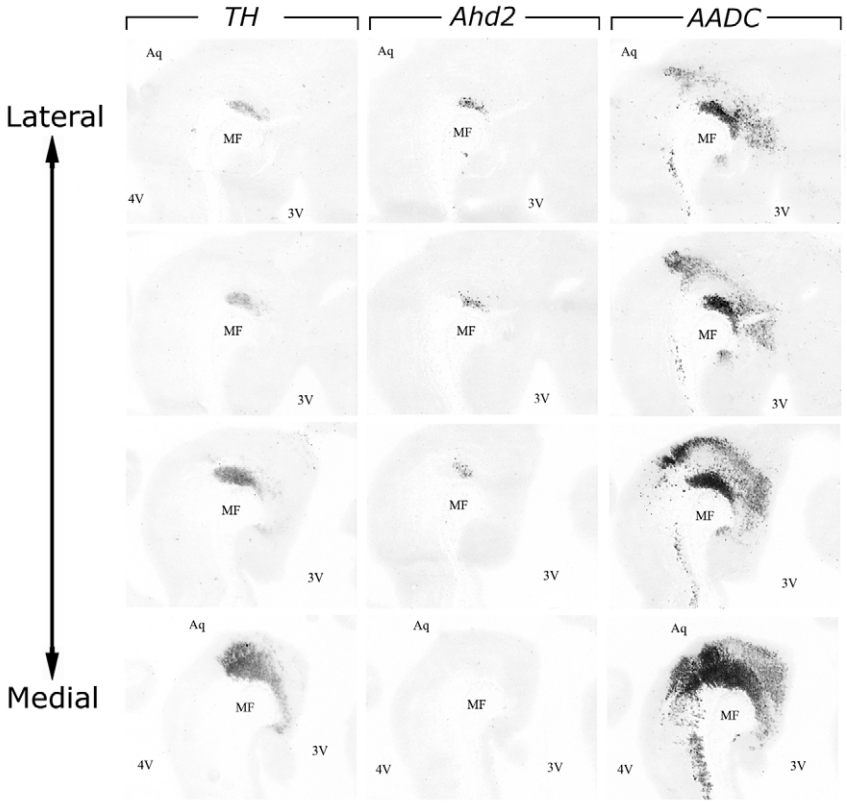

Fig. 2. *Ahd2* expression is restricted to the lateral part of the mdDA during the late differentiation phase. Distribution of *Ahd2* mRNA in sagittal E13.5 sections from the lateral to medial part of the meso-diencephalic dopaminergic (mdDA) area containing neurons in the presumptive substantia nigra pars compacta (SNc) and ventral tegmental area (VTA), respectively. The cell bodies of the fully differentiated mdDA neurons were identified by *Th* mRNA expression, and *Ahd2* expression was analyzed on the adjacent sections. Expression of *Aadc* on the adjacent sections identified, in addition to the fully differentiated mdDA neurons, young migrating DA neurons located more dorsally. 3V, third ventricle; 4V, fourth ventricle; Aq, aqueduct; MF, mesencephalic flexure.

overlap completely. In particular, *Th*+ cells in the medial part of the SNc and dorso-medial part of the VTA appeared to lack *Ahd2* expression. *Ahd2* in situ hybridization (ISH) combined with an immunohistochemical staining for TH clearly confirmed that not all TH+ neurons in the adult SNc and VTA co-expressed *Ahd2* (Fig. 1B). In the lateral tip of the SNc, TH+ cells that did not express *Ahd2* were intermingled with TH+ cells that did express *Ahd2* (Fig. 1BB). In the more medial part of the SNc, TH+ cells that lacked *Ahd2* expression were predominantly located dorsally (Fig. 1BC). In addition, in the VTA, TH+ cells that lacked *Ahd2* expression were mainly observed in the dorsal VTA (Fig. 1BD-BF). Finally, antibody double-labeling experiments assured the subpopulation-specific distribution of Ahd2 protein in the SNc (Fig. 1CA-CC,CG-CI) and VTA (Fig. 1CD-CF,CJ-CL). Not all TH+ cells in the SNc and VTA expressed Ahd2 protein, but those cells that did express Ahd2 protein were all TH+, indicating that Ahd2 and TH are co-expressed in a specific mdDA subpopulation. Taken together, based on both transcript and protein distribution, Ahd2 marks a specific mdDA subpopulation in the adult brain.

It has been reported previously that Ahd2 expression is a marker for proliferating and differentiating mesencephalic DA cells that becomes progressively more restricted during late differentiation and the postnatal stages (McCaffery and Drager, 1994; Wallen et al., 1999). To study the developmental expression of *Ahd2* during late differentiation in more detail, the distribution of *Ahd2* mRNA was examined in E13.5 wild-type embryos (Fig. 2). *Ahd2* expression was confined to neurons located in the more lateral parts of the mdDA area, as identified by the expression of *Th* mRNA on adjacent sections (Fig. 2). Aadc-positive young migrating neurons, which are located more dorsally (Smidt et al., 2004a), and proliferating cells in the ventricular zone did not express Ahd2 at this time point. These data indicate that, at E13.5, *Ahd2* expression is restricted to a specific subpopulation of mdDA neurons located in the lateral part of the mdDA area. By contrast, the medial part of the mdDA area was devoid of *Ahd2* expression. Clearly, *Ahd2* shows mdDA subpopulation-specific expression, indicating that mdDA subpopulations are already specified during development.

Ahd2 expression in *Pitx3*-deficient mdDA neurons

The expression pattern of Ahd2 described above, appears to identify the neuronal subset that is lost in *Pitx3*-deficient animals. To study that possibility in detail, we analyzed the expression of Ahd2 in adult brain and during the late differentiation phase in E13.5 mdDA neurons of *Pitx3*-deficient mice (Fig. 3). The expression pattern of *Th* revealed the previously reported malformation of the adult mdDA system in *Pitx3*-deficient mice (Smidt et al., 2004b), characterized by neuronal loss predominantly in the SNc (Fig. 3A). As expected, *Ahd2* expression was completely absent in the rostral part of the mdDA area of adult *Pitx3*-deficient mice, which includes the SNc and lateral part of the VTA, as identified by the expression of *Th* mRNA on adjacent sections (Fig. 3AA-AD). By contrast, in the caudal part of the mdDA area, some *Ahd2*+ neurons could still be observed in the VTA (Fig. 3AE,AF). Antibody double-labeling experiments demonstrated that the Ahd2+ neurons co-expressed TH protein, indicating that these cells are DA neurons (see Fig. S1 in the supplementary material). At E13.5, *Ahd2* expression was completely lost in the lateral part of the *Pitx3*-deficient mdDA area, which is normally positive for *Ahd2*. By contrast, *Th* expression in adjacent sections was still observed, indicating that there were still mdDA neurons present in this area (Fig. 3B). Taken together, these data clearly demonstrate that *Ahd2* expression is highly affected in *Pitx3*-deficient mice, already early in development.

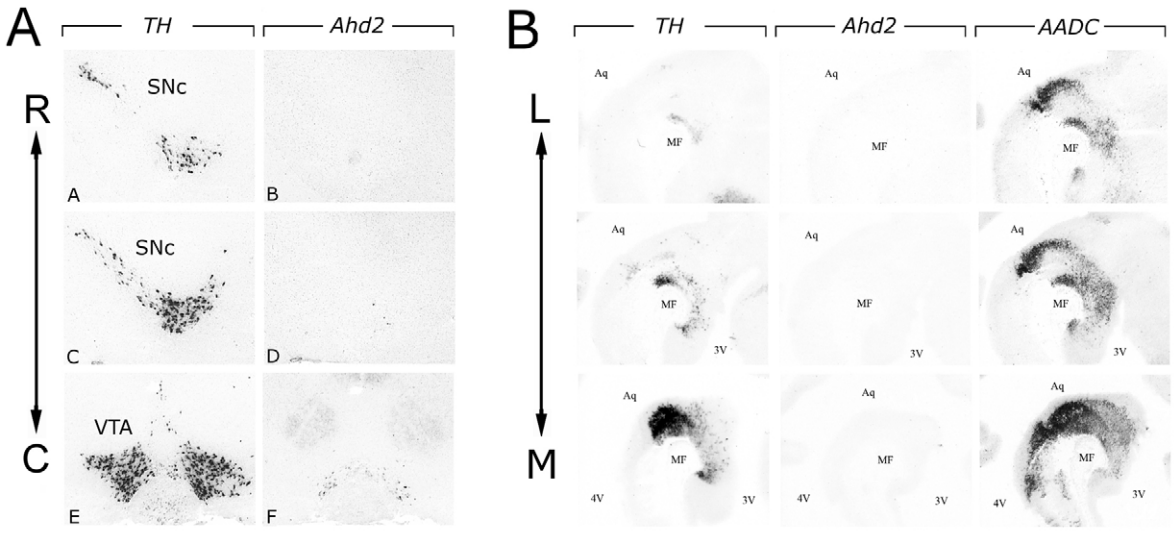

Fig. 3. Ahd2 expression is largely lost in the mdDA system of *Pitx3*-deficient mice. (**A**) Distribution of *Ahd2* in adult coronal sections of *Pitx3*-deficient mice from the rostral (R) to the caudal (C) mdDA area containing neurons in the SNc and VTA. The cell bodies of these mdDA neurons were identified by *Th* mRNA expression (A,C,E), and *Ahd2* expression was analyzed on adjacent sections (B,D,F). (**B**) Distribution of *Ahd2* mRNA in sagittal E13.5 sections from the lateral (L) to medial (M) part of the mdDA area of *Pitx3*-deficient mice. The cell bodies of the fully differentiated mdDA neurons were identified by *Th* mRNA expression, and *Ahd2* expression was analyzed on adjacent sections. Expression of *Aadc* on adjacent sections identified, in addition to the fully differentiated mdDA neurons, young migrating DA neurons located more dorsally. 3V, third ventricle; 4V, fourth ventricle; Aq, aqueduct; mdDA, meso-diencephalic dopaminergic; MF, mesencephalic flexure; SNc. substantia nigra pars compacta; VTA, ventral tegmental area.

Decreased *Ahd2* expression in mdDA neurons of *Pitx3*$^{+/-}$ mice

The apparent loss of *Ahd2* expression in *Pitx3*-deficient mdDA neurons during development suggests that Pitx3 is involved in *Ahd2* gene activation. To study this in more detail, we analyzed the *Ahd2* expression level in *Pitx3*$^{+/-}$ mice, which display reduced *Pitx3* expression (Rieger et al., 2001). We performed quantitative radioactive ISH studies on coronal adult mdDA sections of *Pitx3*$^{+/-}$ mice containing the SNc (Fig. 4). *Ahd2* mRNA levels in the SNc of *Pitx3*$^{+/-}$ mice (Fig. 4, black bar; n=5) were significantly decreased compared with *Pitx3*$^{+/+}$ mice (Fig. 4, white bar; n=8; P<0.05). Expression levels of other mdDA markers, including *Th*, *Vmat2* and alpha-synuclein were not altered in *Pitx3*$^{+/-}$ mice. The fact that *Ahd2* expression was specifically decreased in *Pitx3*$^{+/-}$ mice strongly indicates a dose-dependent effect of Pitx3 on the expression level of *Ahd2*.

Pitx3 regulates *Ahd2* expression in MN9D dopaminergic cells

To investigate further whether Pitx3 regulates *Ahd2* gene transcription, we analyzed whether *Ahd2* expression is influenced by Pitx3 in the DA cell line MN9D. This cell line expresses a multitude of DA markers, and Nurr1 (also known as Nr4a2 – Mouse Genome Informatics) overexpression results in increased levels of DA-related genes, such as *Th*, *Vmat2* and *Aadc* (Hermanson et al., 2003). In addition, Nurr1 induces morphological differentiation and cell cycle arrest (Castro et al., 2001). Therefore, we argued that this cell line is an appropriate cell model in which to analyze Pitx3 function. Under normal conditions, *Pitx3* and *Ahd2* were both expressed endogenously in MN9D cells, albeit at a very low level (Fig. 5A). However Pitx3 overexpression led to a drastic increase in endogenous *Ahd2* transcript levels, whereas the control gene, TATA box binding protein (*Tbp*), showed no alteration in expression levels (Fig. 5A,B). To confirm that the upregulated gene was *Ahd2* and not

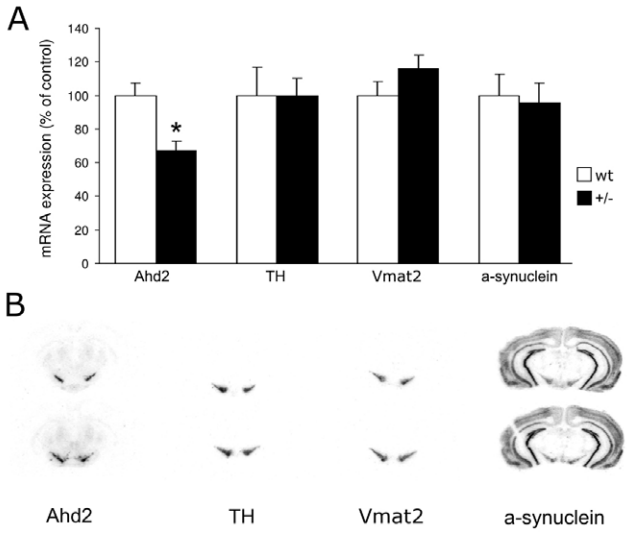

Fig. 4. Expression of *Ahd2* is decreased in SNc mdDA neurons of *Pitx3*$^{+/-}$ mice. (**A**) Quantitative in situ hybridization analysis of the *Ahd2*, *Th*, *Vmat2* and *a-synuclein* mRNA expression levels in the substantia nigra pars compacta (SNc) of *Pitx3*$^{+/+}$ (wt, white bars, n=8) and *Pitx3*$^{+/-}$ (black bars, n=5) mice. The graphs represent the average labeling expressed as percentage of levels in *Pitx3*$^{+/+}$ mice ±s.e.m. and were analyzed by using the Student's t-test (*, P<0.05). (**B**) Typical examples of individual autoradiographic film labeling from coronal sections through the meso-diencephalic dopaminergic (mdDA) area containing the SNc from adult wild-type mice, which were used for determination of mRNA levels.

Aldh1a7, as was the case in vivo (see above), we performed sequence analysis on cloned PCR fragments, revealing that the majority of transcripts (88%) were encoded by the *Ahd2* gene (data

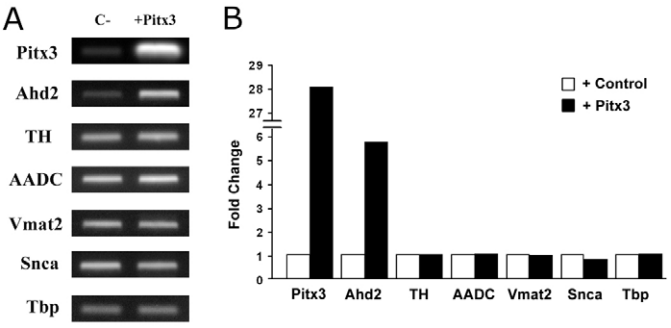

Fig. 5. Effect of Pitx3 overexpression on endogenous *Ahd2* transcript levels and other mdDA marker genes.
(**A**) Overexpression of *Pitx3* in MN9D cells leads to an increase of endogenous *Ahd2* transcript levels. Expression of *Th*, *Aadc*, *Vmat2*, *Snca* and *Tbp* were unaffected. (**B**) Densitometer-based quantification showing the fold change of endogenous transcripts between cells transfected with empty expression vector (+ Control, white bars) and *Pitx3* transfected cells (+ Pitx3, black bars).

not shown). In addition, Pitx3 overexpression showed no effect on the transcript levels of other DA markers, including *Th*, *Aadc*, *Vmat2* and alpha-synuclein (Fig. 5A,B). In total, three independent RNA samples were analyzed, which all gave similar results. These data demonstrate that endogenous *Ahd2* expression largely relies on Pitx3 function, whereas Pitx3 has no effect on the expression of genes involved in neurotransmitter phenotype in these cells.

Pitx3 binds to a highly conserved region in intron 1 of the *Ahd2* gene

The drastic increase in *Ahd2* transcript levels by Pitx3 overexpression may be mediated via direct transcriptional regulation. To investigate whether Pitx3 can bind to enhancer elements within the *Ahd2* promoter, we performed a ChIP assay using specific Pitx3 antibodies. First, we compared rat and mouse *Ahd2* promoter regions ranging from 10 kb upstream to 10 kb downstream of the transcriptional start site (TSS). Because the exact position of the TSS of the mouse *Ahd2* gene is not specified, we compared several expressed sequence tag (EST) sequences, picked the sequence that was found at the 5′ end of many of the transcripts and regarded that sequence as the +1 position. We identified multiple conserved regions containing consensus and non-consensus putative Pitx3-binding sites, and designed primers to amplify those regions that contained fully conserved putative Pitx3-binding sites in both rat and mice. For the analysis, we selected the following mouse genomic regions either upstream (–) or downstream (+) of the TSS: region 1 (–8455 to –8283 bp), region 2 (–4374 to –4252 bp), region 3 (–2981 to –2838 bp), region 4 (+1829 to +1989 bp), region 5 (+2080 to +2181 bp), region 6 (+4204 to +4330 bp), region 7 (+6478 to +6615 bp), region 8 (+6785 to +6941 bp) and region 9 (+7640 to +7765). Next, MN9D cells were transfected with *Pitx3* expression vector to be analyzed in a ChIP-assay. Chromatin was subjected to immunoprecipitation with either αPitx3 antibodies or non-specific rabbit immunoglobulins (IgG). The immunoprecipitated DNA fragments were subjected to PCR, including IgG immunoprecipitated DNA as a negative control and input chromatin as a positive control. Region 2 (Fig. 6A) contains a putative Pitx3-binding site that has been shown to be bound by Pitx3 in an electro mobility shift assay (EMSA) (Chung et al., 2005). In our assay, however, we observed no amplification of this region, indicating that, under the conditions we used, Pitx3 is not bound to that region. This difference can be explained by the use of different approaches to determine functional interactions of a transcription factor to a presumed binding site. It should be noted that, in contrast to a ChIP assay, the chromatin structure in living cells, which can strongly reduce accessibility for transcription factors, is disregarded in an EMSA approach. Interestingly, we successfully amplified a highly conserved genomic region (region 5) specifically from αPitx3 immunoprecipitated DNA (Fig. 6A,B), whereas no amplification of any of the other selected conserved regions was observed (data not shown). The genomic region 4, which lies further upstream than region 5 (Fig. 6A) and shows moderate sequence conservation between rat and mouse, but contains the consensus Pitx3-binding site TAATCC (Wilson et al., 1996), was not amplified (Fig. 6B). This implies selective binding of Pitx3 to the highly conserved region 5. Confirmation of the observed results in a second independent ChIP assay assured selective binding of Pitx3 to region 5. Furthermore, closer analysis of this highly conserved region revealed that, although sequence conservation between mouse/rat and human is generally poor in introns of *Ahd2* (approximately 60%), the homology in this specific intronic region is 91% over a stretch of 60 bp (Fig. 6C). In addition, a non-consensus putative Pitx3-binding site, AAATCT (Wilson et al., 1996; Yuan et al., 1999), which is fully conserved between mouse, rat and human, is found in this region. Altogether, these data indicate that Pitx3

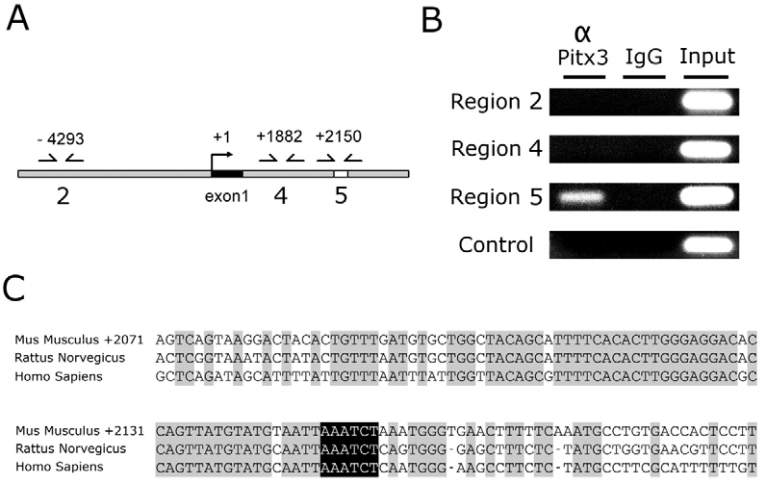

Fig. 6. Pitx3 specifically interacts with a highly conserved region in proximity of the *Ahd2* transcription start site. (**A**) Genomic positions of a selection (regions 2, 4 and 5) of the conserved putative Pitx3-binding sites that were selected for PCR-based analysis in a ChIP assay. (**B**) ChIP assay with either Pitx3 antibody or control rabbit immunoglobulins (IgG), with input chromatin as positive control. Genomic region 5 is specifically amplified from the Pitx3 ChIP sample. No amplification was observed for the previously described Pitx3-binding site (region 2) (Chung et al., 2005) or genomic region 4. Also, a randomly chosen genomic region (Control) showed no amplification. (**C**) Comparison of genomic region 5 between mouse, rat and human, showing high sequence conservation (gray) and a fully conserved non-consensus putative Pitx3-binding site amongst species (black).

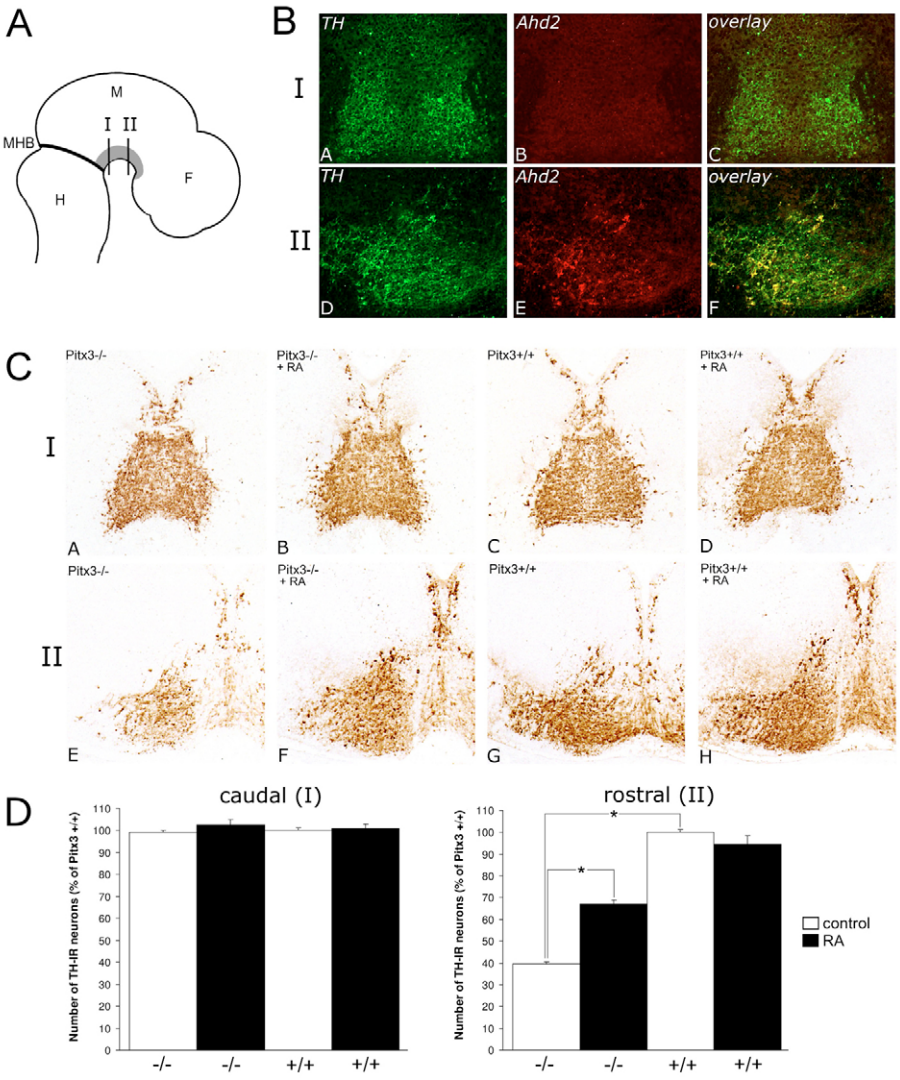

Fig. 7. Retinoic acid treatment counteracts the developmental mdDA defects in *Pitx3* deficiency. (**A**) Schematic representation of an E14.5 sagittal section showing the position of the caudal (I) and rostral (II) sections shown in B and C. The position of the meso-diencephalic dopaminergic (mdDA) neurons are depicted in gray. (**B**) E14.5 coronal sections of the caudal (A-C) and rostral (D-F) part of the mdDA area. (B,E) Ahd2 protein distribution (red). MdDA neurons were identified by the expression of TH protein (green; A,D). Overlays demonstrate the co-expression of the TH and Ahd2 proteins in a specific subpopulation of mdDA neurons located in rostro-lateral positions and defining the developing substantia nigra pars compacta (SNc; C,F). (**C**) Distribution of TH-immunoreactive (TH-IR) neurons in E14.5 coronal brain sections of retinoic acid (RA)-treated Pitx3$^{-/-}$ embryos (B,F), RA-treated *Pitx3*$^{+/+}$ embryos (D,H), untreated *Pitx3*$^{-/-}$ embryos (A,E) and untreated *Pitx3*$^{+/+}$ embryos (C,G) at the caudal (A-D) and rostral (E-H) level of the mdDA area. (**D**) Quantitative analysis of TH-IR neurons in the caudal and rostral part of the mdDA area in RA-treated (black bars) and untreated (white bars) embryos. The average number of TH-IR neurons per section are expressed as a percentage of the number of *Pitx3*$^{+/+}$ embryos ±s.e.m. (n=3; Student's t-test; *P<0.01). F, forebrain; H, hindbrain; M, midbrain; MHB, mid/hindbrain border.

interacts with a highly conserved region 2.1 kb downstream of the TSS of the *Ahd2* gene, which may account for the observed regulation of *Ahd2* gene transcription in MN9D cells.

RA treatment counteracts developmental defects caused by *Pitx3* deficiency

RA generated by aldehyde dehydrogenases is crucial for morphogenesis and cellular differentiation in early eye development. Developmental defects of the eye caused by *Raldh2* deficiency can be effectively rescued by maternal supplementation of synthetic RA during the period when endogenous RA is crucial for proper optic cup formation (Mic et al., 2002; Mic et al., 2004; Molotkov et al., 2006). Ahd2 is a potent generator of RA and is present in the mdDA area throughout embryonic development (Hsu et al., 1999; Haselbeck et al., 1999; Wallen et al., 1999). This suggests a possible role for Ahd2 at this stage of mdDA neuronal development in the synthesis of RA. With *Ahd2* under the transcriptional control of Pitx3, it is appealing to hypothesize that the developmental defect in *Pitx3*-deficient mice is due to a loss of RA synthesis. If RA is crucial for proper development of Ahd2+ neurons in the mdDA system, we could bypass the necessity of *Pitx3*-mediated Ahd2 expression in these neurons by maternal dietary RA administration. Because Ahd2 is expressed in a subset of mdDA neurons, we expected a compensating effect of RA exclusively in that subpopulation. To identify the Ahd2+ mdDA subpopulation at E14.5, when the mdDA phenotype is clearly visible in *Pitx3*-deficient mice (Smidt et al., 2004a; Smidt et al., 2004b; Maxwell et al., 2005), we analyzed Ahd2 expression in wild-type brain at this stage. Ahd2 expression was not detected in caudal sections of the mdDA area, where, ultimately, the VTA is formed (Fig. 7BA-BC). In rostral sections, Ahd2 fully co-localized with TH in a specific subset of TH-immunoreactive (TH-IR) neurons (Fig. 7BD-BF). Ahd2 was predominantly present in mdDA neurons in lateral and ventral positions. The majority of TH-IR neurons in dorso-medial positions did not co-express Ahd2. In addition, TH-IR neurons in a distinct population in most lateral positions were largely negative for Ahd2.

To determine whether RA synthesis by Ahd2, mediated via Pitx3, has a role in the development of these Ahd2+ neurons, we aimed to compensate for *Pitx3* deficiency by maternal dietary RA administration. Pregnant *Pitx3*$^{+/-}$ mice were supplemented with RA from E10.75 to E13.75, and *Pitx3*$^{+/+}$ and *Pitx3*$^{-/-}$ littermates were analyzed at E14.5. Detailed analysis showed that, in caudal regions of the mdDA area, no effect of RA treatment is observed in either the *Pitx3*$^{+/+}$ or *Pitx3*$^{-/-}$ embryos (Fig. 7CA-CD; Fig. 7D, left panel).

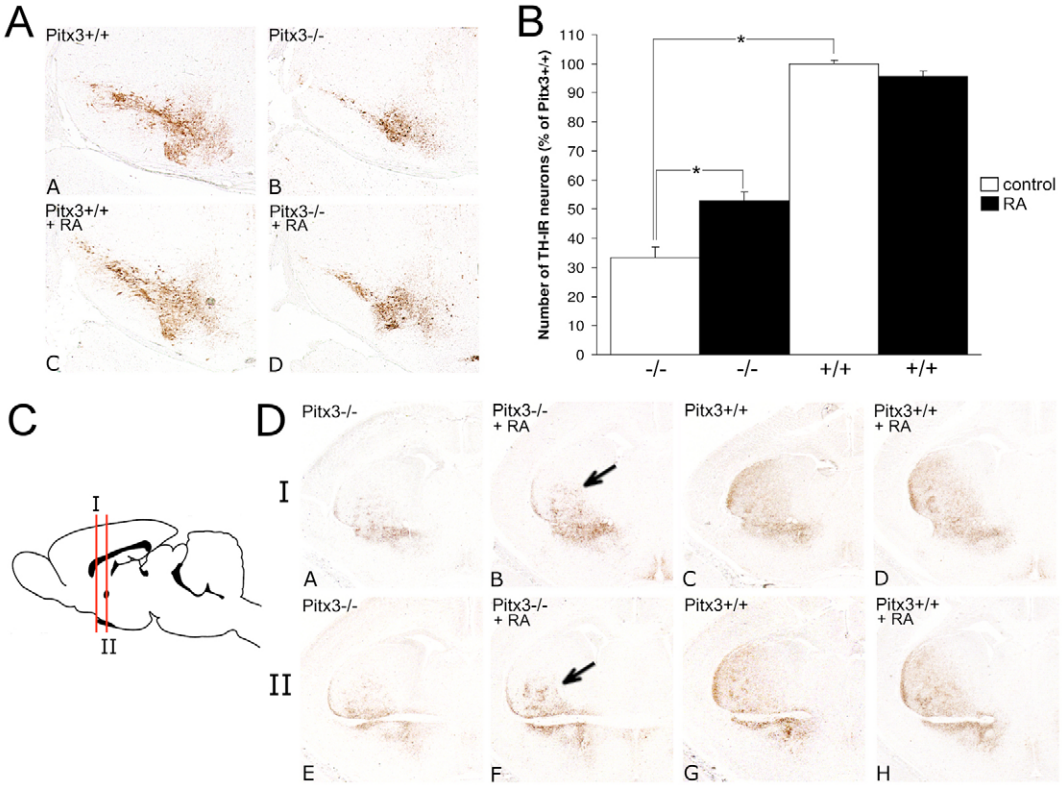

Fig. 8. The effect of temporary retinoic acid treatment in *Pitx3*$^{-/-}$ embryos is maintained at later developmental stages. (**A**) Distribution of TH-immunoreactive (TH-IR) neurons in E18.5 coronal brain sections at the level of the substantia nigra pars compacta (SNc) of untreated *Pitx3*$^{+/+}$ embryos (A), untreated *Pitx3*$^{-/-}$ embryos (B), retinoic acid (RA)-treated *Pitx3*$^{+/+}$ embryos (C) and RA-treated *Pitx3*$^{-/-}$ embryos (D). (**B**) Quantitative analysis of TH-IR neurons in the SNc of E18.5 RA-treated (black bars) and untreated (white bars) embryos. The average number of TH-IR neurons per section are expressed as percentage of the number of *Pitx3*$^{+/+}$ embryos ±s.e.m. (n=3 for untreated *Pitx3*$^{-/-}$, RA treated *Pitx3*$^{-/-}$ and RA-treated *Pitx3*$^{+/+}$ embryos; n=2 for untreated *Pitx3*$^{+/+}$ embryos; Student's t-test; *$P \leqslant 0.01$). (**C**) Schematic representation of an E18.5 sagittal section showing the position of the striatal regions (I and II) demonstrated in D. (**D**) TH-immunoreactivity at two levels of the striatum of E18.5 embryos. The arrows mark the dorsal striatal areas in which an increase of TH-immunoreactivity is observed.

In *Pitx3*$^{+/+}$ embryos, RA treatment had no effect on the occurrence of mdDA neurons in the rostral regions (Fig. 7CG,CH; Fig. 7D, right panel). As previously reported (Smidt et al., 2004a), untreated *Pitx3*$^{-/-}$ embryos displayed a significant loss (61%; n=3, P<0.01) of TH-IR neurons in the ventro-lateral regions (Fig. 7CE,CG; Fig. 7D, right panel). Strikingly, in rostral sections of *Pitx3*$^{-/-}$ embryos, RA treatment led to a significant increase (70%; n=3, P<0.01) in number of TH-IR neurons (Fig. 7CE,CF; Fig. 7D, right panel). As a result, the loss in number of TH-IR neurons caused by *Pitx3* deficiency was drastically reduced after RA treatment. This demonstrates that RA treatment has an exclusive effect in *Pitx3*$^{-/-}$ embryos, affecting specifically the rostral mdDA subpopulation, which is most affected by *Pitx3* deficiency.

In order to understand the nature of the observed rescue effect, we performed Nissl staining to quantify the average amount of neurons per section in the rostral E14.5 mdDA area (n=3; *Pitx3*$^{-/-}$, untreated: 394±18; *Pitx3*$^{-/-}$, RA-treated: 391±36; *Pitx3*$^{+/+}$, untreated: 404±52; *Pitx3*$^{+/+}$, RA-treated: 380±45). No statistical difference in neuronal number was found between all groups, which indicates that, at E14.5, no neurons are lost in either RA-treated or untreated *Pitx3*$^{-/-}$ embryos, compared with *Pitx3*$^{+/+}$ embryos. Furthermore, RA is unable to induce TH expression in MN9D cells (data not shown), which suggests that the observed increase in TH-IR neurons is not due to a general induction of TH expression.

To determine whether the effect of temporary RA treatment is maintained at later developmental stages, we treated pregnant *Pitx3*$^{+/-}$ mice with RA from E10.75 until E13.75 and analyzed *Pitx3*$^{+/+}$ and *Pitx3*$^{-/-}$ littermate embryos at E18.5 (Fig. 8). RA-treated *Pitx3*$^{-/-}$ embryos showed a significant increase in number of TH-IR neurons (59%; n=3, P=0.01) within the SNc. These data indicate that temporary RA treatment has a sustained effect on the mdDA neuronal population. In agreement with the E14.5 data, the effect was highly restricted to *Pitx3*$^{-/-}$ embryos (Fig. 8A,B).

Pitx3$^{-/-}$ mice are characterized by impaired innervation of the dorsal striatum. To determine whether the increased number of TH-IR neurons in RA-treated E18.5 *Pitx3*$^{-/-}$ embryos was accompanied by increased innervation, we analyzed TH-immunoreactivity in dorsal regions of the striatum at multiple levels (Fig. 8C,D). Interestingly, increased TH-immunoreactivity was observed in dorsal regions of the striatum in RA treated *Pitx3*$^{-/-}$ embryos, whereas this area was largely devoid of TH-immunoreactivity in untreated *Pitx3*$^{-/-}$ embryos. These observations indicate that the TH-IR neurons that are maintained in RA-treated *Pitx3*$^{-/-}$ embryos are those neurons that normally innervate striatal regions located more dorsally. Altogether, these data strongly suggest that RA-dependent signaling is essential for the proper development of a specific subset of mdDA neurons initially affected in *Pitx3*-deficient mice.

DISCUSSION

During early developmental stages, the mdDA neuronal population is not homogeneous, but consists of multiple neuronal subpopulations with different temporal and topographical expression patterns (Smits et al., 2006). An early determinant of subset specification is Pitx3 and, based on its temporal expression pattern, two distinct mdDA neuronal populations exist during early development. A ventro-lateral population, which expresses Pitx3 before TH, can be identified, as well as a dorso-medial population, which expresses TH before Pitx3 (Maxwell et al., 2005). The existence of mdDA subpopulations is highlighted by the expression pattern of Ahd2. In the adult brain, we observed Ahd2 expression in a ventrally located subset of TH-IR neurons in the SNc and VTA. During embryonic development, this mdDA subpopulation-specific expression was observed as early as E13.5, showing *Ahd2* expression exclusively in the lateral parts of the mdDA area. The restricted expression of Ahd2 is also clearly visible in the major projection area of the mdDA system, where Ahd2 protein is detected in dorso-lateral parts of the adult striatum (McGaffery and Drager, 1994). Interestingly, innervation to these specific regions of the striatum is lost in *Pitx3*-deficient mice, caused by a selective loss of mdDA neurons predominantly in the SNc. In order to investigate the fate of Ahd2-expressing mdDA neurons in *Pitx3*-deficient mice, we determined the distribution of *Ahd2* transcripts in both the adult and the embryonic brain. Although we observed a small population of mdDA neurons in the ventro-medial part of the VTA that still expressed Ahd2, most of the expression of Ahd2 was completely lost. This indicates that the majority of Ahd2+ mdDA neurons, except for a small distinct population, are fully dependent on Pitx3 expression for proper development. In E13.5 *Pitx3*-deficient embryos, no expression of *Ahd2* was observed in the lateral region of the mdDA area, where the gene is normally expressed. However, *Th* is still expressed in that area, which indicates that a considerable amount of mdDA neurons is still present. Considering the amount of TH+/Ahd2+ cells in wild-type E13.5 embryos, and the amount of remaining TH+ cells in the *Pitx3*-deficient brain, this suggests that loss of Ahd2 expression is due to the ablation of Pitx3 itself rather than to neuronal loss.

The fact that *Pitx3* expression is reduced in *Pitx3*$^{+/-}$ animals (Rieger et al., 2001) provided a tool by which to analyze the in vivo consequence of *Pitx3* gene dosage. Quantitative analysis of *Ahd2* expression in the SNc of *Pitx3*$^{+/-}$ mice revealed a significant reduction in the expression level of *Ahd2*. Expression of other DA marker genes was unaffected in the SNc of *Pitx3*$^{+/-}$ animals, which points to a gene-dosage effect of Pitx3 on *Ahd2* expression specifically, unrelated to neuronal loss. In perfect agreement with these data, we observed a drastic increase in endogenous *Ahd2* transcript levels when Pitx3 was overexpressed in the DA cell line MN9D. This effect was specific for *Ahd2*, because the levels of *Th*, *Aadc*, *Vmat2*, *Tbp* and *alpha-synuclein* were unaffected. Further evidence for the Pitx3-mediated regulation of *Ahd2* transcription was provided via a ChIP assay, which was performed to analyze the binding of Pitx3 to a selection of highly conserved regions in the proximity of the *Ahd2* TSS. We showed that Pitx3 immunoprecipitation specifically selected for a genomic region in intron 1 of the *Ahd2* gene. This region displays a surprisingly high sequence conservation in mouse, rat and human, in contrast to the surrounding intronic sequence of the *Ahd2* gene. A non-consensus putative Pitx3-binding site, AAATCT, is contained within this region, which was also found to be fully conserved.

Because different lines of evidence suggest that Ahd2 is under the transcriptional control of Pitx3, we hypothesized that Ahd2, mediated through Pitx3, might have a role in the development of mdDA neurons. Ahd2 is a potent generator of RA (Hsu et al., 1999; Fan et al., 2003), which is essential for the proper development of many structures in the embryo (Duester et al., 2003), and is involved in neuronal patterning, survival and neurite outgrowth (Clagett-Dame et al., 2006). Although *Ahd2*-deficient animals are viable and exhibit no gross abnormalities, the brain, and, in particular, the mdDA system, have not been analyzed yet (Fan et al., 2003). Although the first step in RA synthesis by alcohol dehydrogenases is an ubiquitous process, tissue specificity of RA synthesis is achieved by restricted expression of aldehyde dehydrogenases, such as Ahd2 (Molotkov et al., 2002). In agreement with the Ahd2 expression pattern, RA is synthesized in the mdDA area during early development, and during the postnatal and adult stages (McGaffery and Drager, 1994; Niederreither et al., 2002a). In this study, we show that maternal supplementation of RA counteracts the developmental defect in the mdDA area in *Pitx3*$^{-/-}$ mice. After RA treatment, a significant increase in the number of TH-IR mdDA neurons was observed in the rostral part of the mdDA system of E14.5 *Pitx3*$^{-/-}$ embryos. This effect was specific to the rostral part of the mdDA system which is the region that is most affected by *Pitx3* deficiency. Importantly, no effect of RA-treatment was observed in *Pitx3*$^{+/+}$ embryos, which rules out the possibility that the observed increase in number of TH-IR neurons is due to increased proliferation. In addition, RA is unable to induce TH expression in MN9D cells, which suggests that the observed increase in TH-IR neurons is not due to a general induction of TH expression. Rather, a possible explanation for the increase in TH-IR neurons is that RA induces the establishment of the proper mdDA identity of immature *Pitx3*$^{-/-}$ neurons. Indeed, previous studies show that, at E14.5, a large population of immature *Pitx3*$^{-/-}$ neurons do not achieve their proper mdDA identity, but are still present in the area as TH-negative neurons (Maxwell et al., 2005). In agreement with these findings, our data indicate that the total number of neurons in the rostral region of the mdDA system is unaffected by either *Pitx3* deficiency or RA treatment. This strongly suggests that the observed decrease of TH-immunoreactivity in E14.5 *Pitx3*$^{-/-}$ embryos is caused by the fact that immature neurons have not established their proper mdDA identity, rather than being lost. Therefore, the increase in the number of TH-IR neurons in RA-treated *Pitx3*$^{-/-}$ embryos appears to be the result of restored mdDA neuronal differentiation.

The effect of the temporary RA treatment was preserved to a comparable level at E18.5, as the number of TH-IR neurons was still significantly increased in RA-treated *Pitx3*$^{-/-}$ embryos. This implies that, for a specific mdDA subset, RA is crucial between E10.75 and E13.75 to induce proper mdDA neuronal identity. Once the correct neuronal identity is established, these neurons appear to be maintained without further RA treatment. Strikingly, the increase in TH-IR number in the mdDA area is accompanied by increased dorsal innervation of the striatum. This strengthens the idea that RA induces the occurrence of a distinct functional mdDA subset in *Pitx3*$^{-/-}$ embryos, which is normally severely affected by *Pitx3*-deficiency.

Altogether, these data indicate that RA can compensate for the loss of Ahd2 expression as a consequence of *Pitx3* deficiency. This positions Ahd2 and its RA-generating potency central in a pathway for mdDA neuronal development, which might be linked to the final differentiation of a specific mdDA neuronal subpopulation. Interestingly, Ahd2 is downregulated in the Parkinsonian SNc, and other components of the RA-synthesis pathway have been correlated to PD (Buervenich et al., 2000; Buervenich et al., 2005; Galter et al.,

2003; Grünblatt et al., 2004). Most appealing, by linking local RA synthesis to mdDA neuronal development and maintenance, a novel mechanism is proposed, with essential implications for clinical pathology as seen in PD.

We would like to thank Thomas Perlmann for kindly providing the MN9D cells, Meng Li for providing the Pitx3$^{+/GFP}$ FACS-sorted cells, and Horst Simon for his kind gift of the Ahd2 fragment.

Supplementary material

Supplementary material for this article is available at
http://dev.biologists.org/cgi/content/full/134/14/2673/DC1

References

Abou-Sleiman, P. M., Muqit, M. M. K. and Wood, N. W. (2006). Expanding insights of mitochondrial dysfunction in Parkinson's Disease. *Nat. Rev. Neurosci.* **7**, 207-219.

Blum, D., Torch, S., Lambeng, N., Nissou, M., Benabid, A. L., Sadoul, R. and Verna, J. M. (2001). Molecular pathways involved in the neurotoxicity of 6-OHDA, dopamine and MPTP: contribution to the apoptotic theory in Parkinson's disease. *Prog. Neurobiol.* **65**, 135-172.

Buervenich, S., Sydow, O., Carmine, A., Zhang, Z., Anvret, M. and Olson, L. (2000). Alcohol dehydrogenase alleles in Parkinson's disease. *Mov. Disord.* **15**, 813-818.

Buervenich, S., Carmine, A., Galter, D., Shahabi, H. N., Johnels, B., Holmberg, B., Ahlberg, J., Nissbrandt, H., Eerola, J., Hellstrom, O. et al. (2005). A rare truncating mutation in ADH1C (G78Stop) shows significant association with Parkinson disease in a large international sample. *Arch. Neurol*. **62**, 74-78.

Castro, D. S., Hermanson, E., Joseph, B., Wallen, A., Aarnisalo, P., Heller, A. and Perlmann, T. (2001). Induction of cell cycle arrest and morphological differentiation by Nurr1 and retinoids in dopamine MN9D cells. *J. Biol. Chem.* **276**, 43277-43284.

Chambon, P. (1996). A decade of molecular biology of retinoic acid receptors. *FASEB J.* **10**, 940-954.

Chung, S., Hedlund, E., Hwang, M., Kim, D., Shin, B.-S., Hwang, D.-Y., Kang, U. J., Isacson, O. and Kim, K.-S. (2005). The homeodomain transcription factor Pitx3 facilitates differentiation of mouse embryonic stem cells into AHD2-expressing dopaminergic neurons. *Mol. Cell. Neurosci.* **28**, 241-252.

Clagett-Dame, M., McNeill, E. M. and Muley, P. D. (2006). Role of all-trans retinoic acid in neurite outgrowth and axonal elongation. *J. Neurobiol*. **66**, 739-756.

Duester, G. (2000). Families of retinoid dehydrogenases regulating vitamin A function: production of visual pigment and retinoic acid. *Eur. J. Biochem.* **267**, 4315-4324.

Duester, G., Mic, F. A. and Molotkov, A. (2003). Cytosolic retinoid dehydrogenases govern ubiquitous metabolism of retinol to retinaldehyde followed by tissue-specific metabolism to retinoic acid. *Chem. Biol. Interact.* **143-144**, 201-210.

Fan, X., Molotkov, A., Manabe, S., Donmoyer, C. M., Deltour, L., Foglio, M. H., Cuenca, A. E., Blaner, W. S., Lipton, S. A. and Duester, G. (2003). Targeted disruption of Aldh1a1 (Raldh1) provides evidence for a complex mechanism of retinoic acid synthesis in the developing retina. *Mol. Cell. Biol*. **23**, 4637-4648.

Galter, D., Buervenich, S., Carmine, A., Anvret, M. and Olson, L. (2003). ALDH1 mRNA: presence in human dopamine neurons and decreases in substantia nigra in Parkinson's disease and in the ventral tegmental area in schizophrenia. *Neurobiol. Dis.* **14**, 637-647.

Grima, B., Lamouroux, A., Blanot, F., Biguet, N. F. and Mallet, J. (1985). Complete coding sequence of rat tyrosine hydroxylase mRNA. *Proc. Natl. Acad. Sci. USA* **82**, 617-621.

Grünblatt, E., Mandel, S., Jacob-Hirsch, J., Zeligson, S., Amariglio, N., Rechavi, G., Li, J., Ravid, R., Roggendorf, W., Riederer, P. et al. (2004). Gene expression profiling of parkinsonian substantia nigra pars compacta; alterations in ubiquitin-proteasome, heat shock protein, iron and oxidative stress regulated proteins, cell adhesion/cellular matrix and vesicle trafficking genes. *J. Neural Transm.* **111**, 1543-1573.

Haselbeck, R. J., Hoffmann, I. and Duester, G. (1999). Distinct functions for Aldh1 and Raldh2 in the control of ligand production for embryonic retinoid signaling pathways. *Dev. Genet.* **25**, 353-364.

Hermanson, E., Joseph, B., Castro, D., Lindqvist, E., Aarnisalo, P., Wallen, A., Benoit, G., Hengerer, B., Olson, L. and Perlmann, T. (2003). Nurr1 regulates dopamine synthesis and storage in MN9D dopamine cells. *Exp. Cell Res.* **288**, 324-334.

Hirsch, E. C., Graybiel, A. M. and Agid, Y. A. (1988). Melanized dopaminergic neurons are differentially susceptible to degeneration in Parkinson's disease. *Nature* **334**, 345-348.

Hsu, L. C., Chang, W. C., Hoffmann, I. and Duester, G. (1999). Molecular analysis of two closely related mouse aldehyde dehydrogenase genes: identification of a role for Aldh1, but not Aldh-pb, in the biosynthesis of retinoic acid. *Biochem. J.* **339**, 387-395.

Hwang, D. Y., Ardayfio, P., Kang, U. J., Semina, E. V. and Kim, K. S. (2003). Selective loss of dopaminergic neurons in the substantia nigra of Pitx3-deficient aphakia mice. *Brain Res. Mol. Brain Res.* **114**, 123-131.

Matthews, J., Wihlen, B., Thomsen, J. and Gustafsson, J. A. (2005). Aryl hydrocarbon receptor-mediated transcription: ligand-dependent recruitment of estrogen receptor alpha to 2,3,7,8-tetrachlorodibenzo-p-dioxin-responsive promoters. *Mol. Cell. Biol.* **25**, 5317-5328.

Maxwell, S. L., Ho, H. Y., Kuehner, E., Zhao, S. and Li, M. (2005). Pitx3 regulates tyrosine hydroxylase expression in the substantia nigra and identifies a subgroup of mesencephalic dopaminergic progenitor neurons during mouse development. *Dev. Biol.* **282**, 467-479.

McCaffery, P. and Drager, U. C. (1994). High levels of a retinoic acid-generating dehydrogenase in the meso-telencephalic dopamine system. *Proc. Natl. Acad. Sci. USA* **91**, 7772-7776.

McCaffery, P. J., Adams, J., Maden, M. and Rosa-Molinar, E. (2003). Too much of a good thing: retinoic acid as an endogenous regulator of neural differentiation and exogenous teratogen. *Eur. J. Neurosci.* **18**, 457-472.

Mic, F. A., Haselbeck, R. J., Cuenca, A. E. and Duester, G. (2002). Novel retinoic acid generating activities in the neural tube and heart identified by conditional rescue of Raldh2 null mutant mice. *Development* **129**, 2271-2282.

Mic, F. A., Molotkov, A., Benbrook, D. M. and Duester, G. (2003). Retinoid activation of retinoic acid receptor but not retinoid X receptor is sufficient to rescue lethal defect in retinoic acid synthesis. *Proc. Natl. Acad. Sci. USA* **100**, 7135-7140.

Mic, F. A., Molotkov, A., Molotkova, N. and Duester, G. (2004). Raldh2 expression in optic vesicle generates a retinoic acid signal needed for invagination of retina during optic cup formation. *Dev. Dyn.* **231**, 270-277.

Molotkov, A., Fan, X., Deltour, L., Foglio, M. H., Martras, S., Farres, J., Pares, X. and Duester, G. (2002). Stimulation of retinoic acid production and growth by ubiquitously expressed alcohol dehydrogenase Adh3. *Proc. Natl. Acad. Sci. USA* **99**, 5337-5342.

Molotkov, A., Molotkova, N. and Duester, G. (2006). Retinoic acid guides eye morphogenetic movements via paracrine signaling but is unnecessary for retinal dorsoventral patterning. *Development* **133**, 1901-1910.

Montplaisir, V., Lan, N. C., Guimond, J., Savineau, C., Bhat, P. V. and Mader, S. (2002). Recombinant class I aldehyde dehydrogenases specific for all-trans- or 9-cis-retinal. *J. Biol. Chem.* **277**, 17486-17492.

Moore, D. J., West, A. B., Dawson, V. L. and Dawson, T. M. (2005). Molecular pathophysiology of Parkinson's disease. *Annu. Rev. Neurosci*. **28**, 57-87.

Niederreither, K., Vermot, J., Fraulob, V., Chambon, P. and Dolle, P. (2002a). Retinaldehyde dehydrogenase 2 (RALDH2)- independent patterns of retinoic acid synthesis in the mouse embryo. *Proc. Natl. Acad. Sci. USA* **99**, 16111-16116.

Niederreither, K., Fraulob, V., Garnier, J. M., Chambon, P. and Dolle, P. (2002b). Differential expression of retinoic acid-synthesizing (RALDH) enzymes during fetal development and organ differentiation in the mouse. *Mech. Dev.* **110**, 165-171.

Niederreither, K., Vermot, J., Schuhbaur, B., Chambon, P. and Dolle, P. (2002c). Embryonic retinoic acid synthesis is required for forelimb growth and anteroposterior patterning in the mouse. *Development* **129**, 3563-3574.

Nunes, I., Tovmasian, L. T., Silva, R. M., Burke, R. E. and Goff, S. P. (2003). Pitx3 is required for development of substantia nigra dopaminergic neurons. *Proc. Natl. Acad. Sci. USA* **100**, 4245-4250.

Rieger, D. K., Reichenberger, E., McLean, W., Sidow, A. and Olsen, B. R. (2001). A double-deletion mutation in the Pitx3 gene causes arrested lens development in aphakia mice. *Genomics* **72**, 61-72.

Semina, E. V., Murray, J. C., Reiter, R., Hrstka, R. F. and Graw, J. (2000). Deletion in the promoter region and altered expression of Pitx3 homeobox gene in aphakia mice. *Hum. Mol. Genet.* **9**, 1575-1585.

Smidt, M. P., van Schaick, H. S., Lanctot, C., Tremblay, J. J., Cox, J. J., van der Kleij, A. A., Wolterink, G., Drouin, J. and Burbach, J. P. (1997). A homeodomain gene Ptx3 has highly restricted brain expression in mesencephalic dopaminergic neurons. *Proc. Natl. Acad. Sci. USA* **94**, 13305-13310.

Smidt, M. P., Asbreuk, C. H., Cox, J. J., Chen, H., Johnson, R. L. and Burbach, J. P. (2000). A second independent pathway for development of mesencephalic dopaminergic neurons requires Lmx1b. *Nat. Neurosci.* **3**, 337-341.

Smidt, M. P., Smits, S. M., Bouwmeester, H., Hamers, F. P. T., van der Linden, A. J. A., Hellemons, A. J. C. G. M., Graw, J. and Burbach, J. P. H. (2004a). Early developmental failure of substantia nigra dopamine neurons in mice lacking the homeodomain gene Pitx3. *Development* **131**, 1145-1155.

Smidt, M. P., Smits, S. M. and Burbach, J. P. H. (2004b). The homeobox gene Pitx3 and its role in the development of dopamine neurons of the substantia nigra. *Cell Tissue Res.* **318**, 35-43.
Smits, S. M., Ponnio, T., Conneely, O. M., Burbach, J. P. and Smidt, M. P. (2003). Involvement of Nurr1 in specifying the neurotransmitter identity of ventral midbrain dopaminergic neurons. *Eur. J. Neurosci.* **18**, 1731-1738.
Smits, S. M., Mathon, D. S., Burbach, J. P., Ramakers, G. M., Smidt, M. P. (2005). Molecular and cellular alterations in the Pitx3-deficient midbrain dopaminergic system. *Mol. Cell. Neurosci.* **30**, 352-363.
Smits, S. M., Burbach, J. P. H. and Smidt, M. P. (2006). Developmental origin and fate of meso-diencephalic dopamine neurons. *Prog. Neurobiol.* **78**, 1-16.
van den Munckhof, P., Luk, K. C., Ste-Marie, L., Montgomery, J., Blanchet, P. J., Sadikot, A. F. and Drouin, J. (2003). Pitx3 is required for motor activity and for survival of a subset of midbrain dopaminergic neurons. *Development* **130**, 2535-2542.
Wallen, A., Zetterstrom, R. H., Solomin, L., Arvidsson, M., Olson, L. and Perlmann, T. (1999). Fate of mesencephalic AHD2-expressing dopamine progenitor cells in NURR1 mutant mice. *Exp. Cell Res.* **253**, 737-746.
Westerlund, M., Galter, D., Carmine, A. and Olson, L. (2005). Tissue- and species-specific expression patterns of class I, III, and IV Adh and Aldh 1 mRNAs in rodent embryos. *Cell Tissue Res.* **322**, 227-236.
Wilson, D. S., Sheng, G., Jun, S. and Desplan, C. (1996). Conservation and diversification in homeodomain-DNA interactions: a comparative genetic analysis. *Proc. Natl. Acad. Sci. USA* **93**, 6886-6891.
Yuan, D., Ma, X. and Ma, J. (1999). Recognition of multiple patterns of DNA sites by Drosophila homeodomain protein Bicoid. *J. Biochem.* **125**, 809-817.
Zhao, S., Maxwell, S., Jimenez-Beristain, A., Vives, J., Kuehner, E., Zhao, J., O'Brien, C., de Felipe, C., Semina, E. and Li, M. (2004). Generation of embryonic stem cells and transgenic mice expressing green fluorescence protein in midbrain dopaminergic neurons. *Eur. J. Neurosci.* **19**, 1133-1140.